

TEMPERATURE DEPENDENCE OF ELECTRON TRANSFER BETWEEN BACTERIOPHEOPHYTIN AND UBIQUINONE IN PROTONATED AND DEUTERATED REACTION CENTERS OF *Rhodopseudomonas sphaeroides*

CRAIG C. SCHENCK AND WILLIAM W. PARSON, *Department of Biochemistry
SJ-70, University of Washington, Seattle, Washington 98195*

DEWEY HOLTEN AND MAURICE W. WINDSOR, *Department of Chemistry,
Washington State University, Pullman, Washington 99164*

AKINORI SARAI, *Department of Physics, Nagoya University, Chikusa-ku, Nagoya,
Japan*

ABSTRACT The rate of the electron-transfer reaction between bacteriopheophytin and the first quinone in isolated reaction centers of *Rhodopseudomonas sphaeroides* has an unusual temperature dependence. The rate increases about threefold with decreasing temperature between 300 and 25 K, and decreases abruptly at temperatures below 25 K. Partial deuteration of the reaction centers alters the temperature dependence of the rate constant. Qualitative features of the temperature dependence can be understood in the context of a theory of nonadiabatic electron transfer (Sarai, 1980. *Biochim. Biophys. Acta.* 589:71–83). We conclude that very low-energy ($10\text{--}50\text{ cm}^{-1}$) processes, perhaps skeletal vibrations of the protein, are important to electron transfer. Higher-energy vibrations, possibly involving the pyrrolic N—H bonds of bacteriopheophytin, also are important in this process.

INTRODUCTION

In photosynthetic bacteria, absorption of a photon promotes the primary electron donor (P, a special dimer of bacteriochlorophylls)¹ to an excited singlet state. An electron is subsequently transferred in ~ 4 ps to a special molecule of bacteriopheophytin, H, probably by way of another bacteriochlorophyll (1, 2). H[•] reduces a quinone (Q) with a rate constant of $\sim 5 \times 10^9\text{ s}^{-1}$ at room temperature (3–5). These electron transfer reactions take place on the scaffolding of a pigment-protein complex known as the reaction center. In *Rhodopseudomonas sphaeroides*, Q is a benzoquinone, ubiquinone; in some other species it is a menaquinone.

The temperature dependence of the electron transfer steps close to the initial photochemical event is one of the most intriguing aspects of the photosynthetic apparatus. Several of these reactions display remarkable non-Arrhenius temperature dependences (6–8). Charge separation to the level of P⁺HQ^{•-} occurs with a quantum yield near unity over the temperature range 4–300 K (9, 10). The rate constant for back reactions between P⁺ and Q^{•-} actually increases by about a factor of 4 if one lowers the temperature from 295 to 4 K (7, 11, 12). If electron

¹Abbreviations used in this paper: H and H[•], oxidized and reduced forms of a special molecule of bacteriopheophytin in the reaction center; P⁺ and P, oxidized and reduced forms of a special dimer of bacteriochlorophylls; Q and Q^{•-}, oxidized and reduced forms of a ubiquinone.

transfer between H^- and Q is blocked, the P^+H^- radical pair formed upon excitation decays in 10–20 ns over a wide temperature span (4–300 K) (13, 14). The observations that both the formation of P^+HQ^- and the competing decay routes for P^+H^- are relatively insensitive to temperature suggest that the reaction $P^+H^-Q \rightarrow P^+HQ^-$ is not strongly temperature dependent. Indeed, it has been reported that the rate of this reaction is independent of temperature from 4 to 295 K (8), but since this study involved measurements at only a small number of temperatures, we thought that a more extensive investigation might be informative.

It is generally accepted that nuclear vibrations in the reactants, products, and solvent molecules are important in assisting electron transfer reactions (14). The substitution of deuterium for hydrogen atoms in the reactants thus can alter rates of electron transfer. In this paper, we examine the effect of temperature on the rate of the reaction $P^+H^-Q \rightarrow P^+HQ^-$ in reaction centers isolated from both partially deuterated bacteria and normal, undeuterated bacteria.

MATERIALS AND METHODS

Reaction centers from *R. sphaeroides* wild type strain 2.4.1 were prepared as described (15). The growth medium for these cells contained ordinary 1H_2O . Reaction centers from *R. sphaeroides* carotenoidless strain R-26 were prepared by a modification of the procedures described by Clayton and Wang (16) and Wraight (17) from cells that had been grown in 1H_2O , and also from cells grown in 2H_2O (Schenck et al., submitted for publication). We shall refer to the deuterated and undeuterated preparations as 2H and 1H reaction centers. The 2H reaction centers were only partially deuterated, because the growth medium contained 1H succinate. These conditions give a nonuniform distribution of 2H in the reaction centers: some positions in the bacteriochlorophyll molecules are almost completely deuterated, and others almost completely undeuterated (18). Any freely exchangeable deuterons would have been replaced by protons during the purification of the reaction centers, because the purification was performed in 1H_2O . The linewidth of the EPR signal of the radical P^+ was measured with a Varian model E-9 instrument (Varian Associates, Inc., Palo Alto, Calif.); it was 9.8 gauss in the 1H R-26 reaction centers and 6.35 G in the 2H R-26 reaction centers.

The picosecond apparatus has been described (1). The 530-nm excitation pulses were 7 ps in duration and ~ 1.4 mm in diameter. The energy of the pulses was 1.5 mJ for the experiments with R-26 reaction centers and somewhat less for the experiments with 2.4.1 reaction centers. Some measurements also were made with 0.2-mJ 600-nm excitation pulses, which were obtained by stimulated Raman scattering in perdeuterocyclohexane. For the experiments with 2.4.1 reaction centers, a homemade liquid-He dewar was used, with an evacuated space surrounding the cuvette, which was mounted on a cold finger. For the experiments with R-26 reaction centers, a Janis model 8DT liquid-He dewar was used (Janis Research Co., Stonham, Mass.); this allowed us to control the temperature continuously by heating the He gas that flowed around the sample. The cuvette was constructed of quartz and sapphire windows sandwiched between two copper plates. A gold (0.7% iron atoms) vs. chromel thermocouple was placed in the copper ~ 2 mm from the optically excited region of the sample.

The picosecond apparatus requires careful imaging of the measuring light on a sample of good optical quality. For experiments at low temperatures we therefore used reaction center samples embedded in polyvinyl alcohol, a water-soluble polymer. This avoided problems associated with cracking in glycerol-buffer glasses. The polyvinyl alcohol films were prepared as follows: 0.6 g polyvinyl alcohol (viscosity = 35–45 cp for a 4% aqueous solution; Polysciences, Inc., Warrington, Pa.) was added to 1.4 ml of 10 mM Tris HCl, pH 8, 0.1% lauryldimethylamine oxide, 100 μ M EDTA (TL buffer) in a 10-ml beaker. The mixture was heated over a flame with vigorous stirring for 30 min, until the polymer was largely dissolved. H_2O was added to make up for evaporative losses, and the extremely viscous white solution was allowed to cool to 20°C. Next, 2 ml of ~ 40 μ M reaction centers in TL buffer was added and

the mixture was stirred at 20°C until it was homogeneous. Air bubbles and a few particles of undissolved polyvinyl alcohol were removed by centrifuging at $2 \times 10^4 g$ for 30 min. 3.0 g of the suspension was poured into a square mold (6.25 cm² in area) constructed from teflon and glass. The open mold was placed in a dark desiccator at 4°C. After several days, >95% of the water had evaporated, leaving a film ~ 0.5 mm thick. The absorbance of the film at 800 nm was ~2. The film was cut into three or four pieces, which were stacked together for study. Conventional absorption spectra of the films were measured with an Aminco-Chance recording spectrophotometer (American Instrument Co., Silver Springs, Md.) The films were essentially nonscattering, both at 295 K and at very low temperatures. The films were stored at -20°C and were stable over a period of many months.

For some of the measurements near 295 K, reaction centers were suspended in TL buffer. In one experiment, we used ¹H R-26 reaction centers that had been dialyzed twice at 295 K in TL buffer made with ²H₂O; all other experiments used ¹H₂O buffer. The reaction center concentrations were typically 8 mM and flash-induced absorbance changes were measured in a 2-mm pathlength cuvette.

We determined the rate constant k for the $P^+H^-Q \rightarrow P^+HQ^-$ reaction by fitting the observed absorbance changes to the function

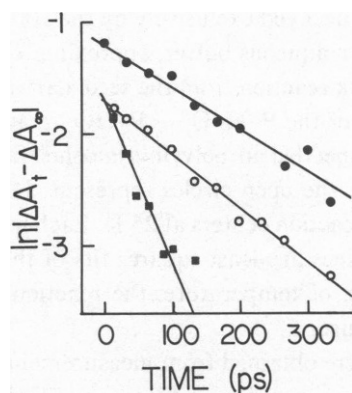


FIGURE 1

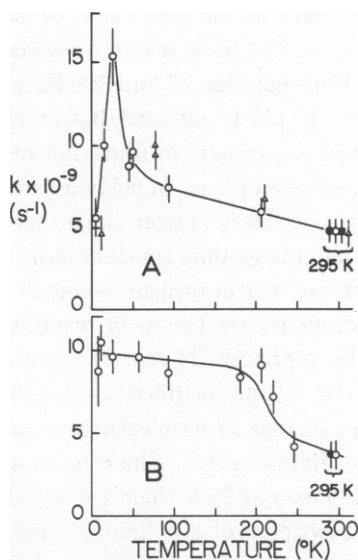


FIGURE 2

FIGURE 1 Decay kinetics of light-induced absorbance changes at 650 nm in reaction centers embedded in polyvinyl alcohol, after excitation at 530 nm. Open circles, ¹H R-26 reaction centers at 295 K; filled circles, ²H R-26 reaction centers at 295 K; filled squares, ¹H R-26 reaction centers at 25 K. Each data point represents the mean of 4–6 measurements of ΔA_t , spaced several minutes apart. The uncertainties of the means were typically ± 0.025 . Solid lines are best fits to the data by a least-squares procedure. Similar measurements (not shown) were made of the absorbance changes at 545 and 680 nm, after 600-nm excitation of ¹H R-26 reaction centers at 295 K; within experimental error, the decay kinetics were identical with those measured at 650 nm after 530-nm excitation.

FIGURE 2 Rate constant (k) for the electron-transfer reaction $P^+H^-Q \rightarrow P^+HQ^-$ as a function of temperature. k was calculated from measurements of absorbance changes at 650 nm, as in Fig. 1. Open symbols are for reaction centers in polyvinyl alcohol, and filled symbols are for reaction centers in TL buffer. (A) Triangles represent ¹H 2.4.1 reaction centers, circles represent ¹H R-26 reaction centers, and the square represents ¹H R-26 reaction centers in ²H₂O TL buffer. (B) ²H R-26 reaction centers. The lengths of the error bars are twice the derived sample standard deviation in k . The curves are drawn to connect the points shown with open symbols, and do not represent theoretical fits.

$$\ln |\Delta A_t - \Delta A_\infty| = \ln |\Delta A_0| - kt,$$

using a least-squares procedure (19). ΔA_t is the absorbance change measured at time t ; ΔA_0 , the initial absorbance change (a fitting parameter); and ΔA_∞ , the residual absorbance change remaining 3–10 ns after the flash. The uncertainty in ΔA_∞ was estimated from the sample standard deviation of 8–10 independent measurements.

RESULTS

To facilitate measurements at low temperatures, we embedded reaction centers in polyvinyl alcohol films. The visible and near infrared absorption spectra of the reaction center films were identical with those of reaction centers in solution. The temperature dependence of the long-wavelength absorption band of P was measured for 2.4.1 reaction centers in polyvinyl alcohol films between 77 and 300 K. The band sharpened and shifted to longer wavelengths with decreasing temperature, as it does with reaction centers in solution (20) or in chromatophores (7). A plot of the absorption maximum vs. temperature was superimposable on the plot that Clayton and Yau (20) have reported for reaction centers in aqueous glycerol. The kinetics of the back reaction between P^+ and Q^- were measured in the 2.4.1 reaction centers in films between 77 and 300 K, and were found to be the same as those that have been measured (11, 12) in glycerol/buffer glasses. The only functional difference we observed between reaction centers in films and reaction centers in aqueous buffer was the amount of active secondary quinone. In polyvinyl alcohol, P^+Q^- decayed exclusively by the 100-ms back reaction that occurs (21) from the primary quinone. In aqueous buffer, approximately half of the decay had the 1-s time constant indicative of a back reaction from the secondary quinone.

Fig. 1 shows typical measurements of the kinetics of the $P^+H^-Q \rightarrow P^+HQ^-$ reaction. All three experiments are for R-26 reaction centers embedded in polyvinyl alcohol films. The filled circles represent 2H reaction centers at 295 K, the open circles represent 1H reaction centers at 295 K, and the filled squares represent 1H reaction centers at 25 K. Each point gives the average of four to six measurements. The solid lines are least-squares fits of the data to exponential decay curves. There is an unusual effect of temperature: the reaction is about three times faster at 25 K than it is at room temperature.

Fig. 2 shows plots of k vs. temperature; the data were obtained from measurements similar to those presented in Fig. 1. Open symbols are for reaction centers in films, and filled symbols are for reaction centers in aqueous solution (TL buffer). Panel A shows data for 1H reaction centers. With 1H R-26 reaction centers, the rate constant increases gradually with decreasing temperature between 300 and 50 K, peaks sharply near 25 K, and decreases abruptly at temperatures below 25 K (open circles in panel A). This effect can be repeated over several cooling/heating cycles in a given sample. Similar results were obtained with 1H 2.4.1 reaction centers (triangles), but the rate constant measured at 80 K was somewhat greater than the line drawn through the data for the R-26 reaction centers. At room temperature, the rate constant is the same for reaction centers in films and in TL buffer. The replacement of 1H_2O by 2H_2O at room temperature has no significant effect on the kinetics (filled square).

Panel B of Fig. 2 shows similar measurements with 2H R-26 reaction centers. At 295 K, partial deuteration of the reaction centers decreases k by ~20% (see also Fig. 1). The rate constant increases rapidly with decreasing temperature in the 2H reaction centers, and becomes greater than that measured with 1H reaction centers in the temperature region

between 50 and 200 K, but it seems to be relatively insensitive to temperature below 200 K. It is unclear whether the rate decreases at very low temperatures, because the uncertainty in the value for k at 4 K is relatively large. Within the experimental error, the rates at 4 and 10 K are the same as that at 25 K. As with the ^1H reaction centers, the rate constant at 295 K is the same in polyvinyl alcohol films and in solution.

DISCUSSION

Peters et al. (8) have reported that the kinetics of the $\text{P}^+\text{H}^-\text{Q} \rightarrow \text{P}^+\text{HQ}^-$ reaction are independent of temperature. They measured the decay at only three temperatures (4, 58, and 295 K), however. In Fig. 2, note that the rate constants that we measured at 4 and 295 K are very similar, so that our results at these temperatures agree with those of Peters et al. The rise and fall of the rate occurs largely in the temperature range between 4 and 58 K. Our method of sample preparation for the low-temperature measurements was different from that of Peters et al., but, with the exception of electron transfer to the second quinone, all of the functional features we examined appeared to be the same in polyvinyl alcohol films as in glycerol/buffer glasses. In addition, the rate constant for the $\text{P}^+\text{H}^-\text{Q} \rightarrow \text{P}^+\text{HQ}^-$ reaction at 295 K is the same in polyvinyl alcohol films as it is in solution, and is unaffected by the substitution of $^2\text{H}_2\text{O}$ for $^1\text{H}_2\text{O}$ (Fig. 2). These observations argue that intramolecular forces are more important in determining the rate of the reaction than are interactions with the polyvinyl alcohol or the aqueous buffer.

According to time-dependent perturbation theory, the rate constant for nonadiabatic electron transfer can be expressed as

$$k = \frac{1}{h} |J|^2 \sum_r \sum_p B_r |\langle \chi_r | \chi_p \rangle|^2 \delta(E_r - E_p). \quad (1)$$

In this expression, the total rate is obtained by summing over all the possible nuclear configurations of the reactants and products, weighting each initial state (r) to achieve the proper thermal average. $|J|^2$ is the square of the matrix element for electron tunneling and is a measure of the electronic orbital overlap between the donor and acceptor molecules. $|J|$ probably decreases exponentially with increasing distance between the two molecules (22, 23). The description of the electron transfer as nonadiabatic means that electronic overlap between the donor and acceptor is relatively weak, which probably is generally the case in biological molecules (22–24). The term $|\langle \chi_r | \chi_p \rangle|^2$ (often called a Franck-Condon factor) is the square of the overlap integral for nuclear wave functions of the reactants (χ_r) and products (χ_p). $B_r = e^{-E_r/kT} / \sum_r e^{-E_r/kT}$ gives the thermal weighting for each initial state. $\delta(E_r - E_p)$, the delta function operating on the energies of the reactants and products, insures the conservation of energy during the electron transfer.

The temperature dependence of the rate of electron transfer reactions is usually ascribed to the weighting factors of the Franck-Condon terms. Deuteration lowers the vibrational frequency of molecular vibrations involving hydrogen atoms, and thus can alter the Franck-Condon terms. The distinct isotope effects on the temperature dependence are consistent with the view that the Franck-Condon weighting factors are responsible for the temperature dependence of the electron transfer in the present case. However, J also could be a function of

temperature, if the orientation or distance between donor and acceptor were sensitive to temperature.

Several attempts have been made to recast Eq. 1 in a form that can be evaluated from experimentally determined parameters. Reviews of this theoretical work appear in references 24 and 25. In a theory developed by Jortner (22, 26), following work by Lax (27) and Kubo and Toyozawa (28), the temperature dependence of the electron transfer rate is expressed in terms of a single vibrational mode in the reactants and products and a low-energy vibration of the solvent. Kakitani and Kakitani (29) have extended the theory to allow for a difference of vibrational frequencies in the reactants and products. These theories have been applied to the reaction between P^+ and a membrane-bound cytochrome in chromatophores of *Chromatium vinosum* (24–29). The rate of cytochrome oxidation is independent of temperature below 120 K (6), which indicates that low-energy vibrations in the reactants are relatively unimportant in this case. Jortner's theory also has been used to discuss the reaction between H^- and Q (8, 22). The theory can account for an increase in rate with decreasing temperature, if the nuclear rearrangement energy ($S\hbar\bar{\omega}$ in Jortner's terminology) is equal to the electronic free energy gap (ΔE) between the reactants and products (22, 25). ($S\hbar\bar{\omega}$ and ΔE are taken to be independent of temperature in Jortner's theory.) A decrease in the temperature from 295 to 4 K, however, is predicted to increase the rate constant by at most 30–40% (22, 25), which is considerably less than the effect that we observed (Fig. 2 A). Larger increases could be explained if the vibrational frequency changes in the reaction, as described by Kakitani and Kakitani (29); such a change makes ΔE temperature dependent. Jortner's theory also would not account for the decrease in the rate at very low temperatures.

The unusual temperature dependence around 25 K seems likely to reflect the thermal activation of very low-frequency vibration modes. Sarai (30, 31) has extended the theory of electron transfer to include an arbitrary number of such low-energy (10–200 cm^{-1}), or “soft,” vibrational modes. The low-energy vibrations could be due to solvent molecules, skeletal vibrations of the protein, or intermolecular or internal motions of the electron carriers (30–32). Each vibration (i) is characterized by a frequency, ω_i , which is assumed to be the same in the reactants and the products, and by a dimensionless coupling strength, S_i . S_i is $x_i^2\mu_i\omega_i/2\hbar$, where x_i is the change that the reaction causes in the mean distance between the vibrating atoms or groups², and μ_i is the reduced mass of the vibrating groups. The inclusion of several soft vibrational modes allows the theory to account for large increases in rate with decreasing temperature and for an abrupt decrease in the rate at very low temperatures.

Fig. 3 shows theoretical curves of the electron-transfer rate as a function of temperature, calculated from Sarai's expression, Eq. 1 of reference 31. In panel A, three vibrational frequencies were used: a relatively high energy, or quantum, mode with $\hbar\omega_1 = 400 \text{ cm}^{-1}$, and two soft modes³ with $\hbar\omega_2 = 50 \text{ cm}^{-1}$ and $\hbar\omega_3 = 10 \text{ cm}^{-1}$. Attempts to fit the data using a smaller number of modes were less successful. The value of S_i for each of the three vibrations

²Note that x_i could describe any change in the equilibrium geometry of the system, and generally does not refer to the distance between the electron donor and acceptor.

³The distinction between quantum modes and soft modes is not a fundamental one. Normal modes with energies higher than $\sim 200 \text{ cm}^{-1}$ are called quantum modes, because their zero-point energy states are dominantly occupied at 300 K.

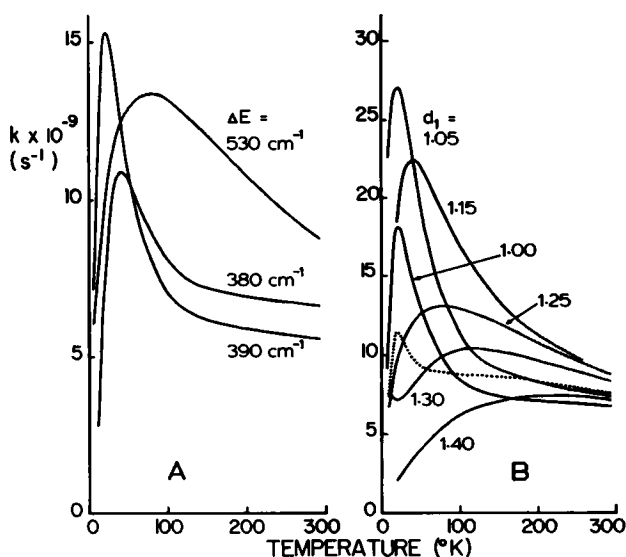


FIGURE 3 Theoretical plots of k as a function of temperature, calculated from Eq. 1 of Ref. 31. (A) $J = \sqrt{10} \text{ cm}^{-1}$; $\hbar\omega_1 = 400 \text{ cm}^{-1}$; $\hbar\omega_2 = 50 \text{ cm}^{-1}$; $\hbar\omega_3 = 10 \text{ cm}^{-1}$; $S_1 = S_2 = S_3 = 1$; ΔE varied as indicated. A positive ΔE means that the reaction is exergonic. (B) $J = \sqrt{10} \text{ cm}^{-1}$; $\hbar\omega_1 = 700/d_1 \text{ cm}^{-1}$; $\hbar\omega_2 = 50/d_2 \text{ cm}^{-1}$; $\hbar\omega_3 = 10 \text{ cm}^{-1}$; $S_1 = d_1$; $S_2 = d_2$; $S_3 = 1.0$; ΔE held constant at 690 cm^{-1} . Solid curves: the deuteration parameter for the quantum mode (d_1) was varied as indicated, with the parameters d_2 and d_3 for the two soft modes fixed at 1.0. Dotted curve: d_2 was set at 1.4, with $d_1 = d_3 = 1.0$.

was arbitrarily set at 1.0, which is a reasonable order of magnitude for bacteriopheophytin and quinones (29, 32). The tunneling matrix element J was fixed at $\sqrt{10} \text{ cm}^{-1}$. This is close to the range of 0.5–2 cm^{-1} that Peters et al. (8) and Jortner (22) used to fit the data of Peters et al. with Jortner's theory. The three curves show the temperature dependence calculated for several values of the electronic energy gap ΔE between reactants and products. The theory predicts a peak in the rate near 25 K, if $\Delta E \approx n\hbar\omega_1$, with n an integer. The curve shown for $\Delta E = 390 \text{ cm}^{-1}$ ($n = 1$) is very similar to the experimental results obtained with ^1H R-26 reaction centers (Fig. 2 A). Similar fits to the data can be obtained with other values of ω_1 and ΔE , or other integral values of n , provided that $\Delta E \approx n\hbar\omega_1$.

The actual value of ΔE for electron transfer from H^- to Q is not well known. Recent measurements of delayed fluorescence from isolated reaction centers indicate that $\text{P}^+\text{H}^-\text{Q}$ lies $\sim 6,000 \text{ cm}^{-1}$ above P^+HQ^- in enthalpy, and $\sim 5,000 \text{ cm}^{-1}$ above it in free energy (33). Earlier calorimetric measurements (34) indicated that the enthalpy change could even be as large as $10,000 \text{ cm}^{-1}$. These values are considerably larger than the value that we used for ΔE in Fig. 3 A (390 cm^{-1}). However, enthalpy and free energy changes calculated from calorimetry or delayed fluorescence may not be directly relevant to the kinetics of the electron transfer reaction, because they reflect equilibrium states of the system. These states may be formed by relatively slow relaxations that occur after the electron transfer reaction. The electron transfer reaction also could involve a low-lying excited electronic state of the products. One can, however, fit the kinetic data using quite large values of ΔE , if one increases the value of J , in addition to n and ω_1 . A curve very similar to the one labeled “ 390 cm^{-1} ” in Fig. 3 A can be

generated by using, for example, the parameters $\Delta E = 8,390 \text{ cm}^{-1}$, $J = 80 \text{ cm}^{-1}$, $\hbar\omega_1 = 1,400 \text{ cm}^{-1}$ ($n = 6$), $\hbar\omega_2 = 50 \text{ cm}^{-1}$, $\hbar\omega_3 = 10 \text{ cm}^{-1}$, and $S_1, S_2, S_3 = 1.0$.

The value of 80 cm^{-1} for J is 1–2 orders of magnitude larger than the values of $0.5\text{--}2 \text{ cm}^{-1}$ that Peters et al. (8) and Jortner (22) used to fit the data of Peters et al. On the assumption that J decreases exponentially with distance, the distance between H^- and Q could be $3\text{--}6 \text{ \AA}$ shorter than the $11\text{--}13 \text{ \AA}$ that Peters et al. and Jortner calculated on the basis of their values for J . Smaller values of J also will fit our data (with ΔE still $\approx 8,000 \text{ cm}^{-1}$) if one increases S_1 , but values of S_1 much greater than 1 are probably not physically realistic (29, 32). Because of the large number of adjustable parameters in the theory, and the uncertainty concerning ΔE , the data do not justify any firm conclusions on the magnitude of J , or on the distance between and H and Q.

Deuteration can affect the rate of electron transfer by changing some of the vibrational frequencies and the corresponding coupling strengths. For a particular vibration (i), replacement of some or all of the ^1H on the vibrating groups by ^2H will increase μ_i by a factor d_i^2 between 1 and 2. This would simultaneously increase S_i and decrease ω_i , both by the factor d_i . In general, d_i cannot be expressed analytically, because it depends on many factors, including the geometry of the system, the masses of all the atoms involved in the vibration, the type of normal mode, and the site and degree of deuteration. We therefore use d_i simply as a parameter that can vary from 1 to $\sqrt{2}$. The solid curves in Fig. 3B show the effect of changing d for the quantum mode (d_1) between 1.0 and $\sqrt{2}$; the dotted curve shows the effect of fixing d_2 at 1.2. Varying d_3 between 1.0 and $\sqrt{2}$ had little effect on the rate (not shown). Some of the curves obtained with d_1 or $d_2 > 1$ resemble the data from deuterated reaction centers (Fig. 2B). Although none of the curves fits the data exactly, the simulations show that it is easy to lose the sharp peak in rate near 25 K and the steep temperature dependence at temperatures below 25 K.

For all of the theoretical curves in Fig. 3B, ΔE was held constant at approximately $\hbar\omega_1$. Under these conditions, the calculated rate constant at high temperatures is not very sensitive to d_1 . The rate even increases slightly with increasing d_1 up to ~ 1.2 . Experimentally, partial deuteration of the reaction centers caused the rate at 295 K to decrease by $\sim 20\%$ (Fig. 2). The theory can account for this effect if ΔE is a higher multiple of $\hbar\omega_1$. This is shown in Fig. 4. For these curves, $\hbar\omega_1$ was fixed at 700 cm^{-1} , as in Fig. 3B, and ΔE was chosen so that $n = 1, 4$, or 6. J was adjusted to keep k approximately constant at $d_1 = 1.0$. With larger values of n , the rate constant at 300 K becomes increasingly sensitive to d_1 . k goes through a maximum when d_1 is slightly greater than 1.0, and then decreases abruptly. The observed effect of deuteration is compatible with values of n on the order of 4–6, but does not allow us to determine n with any accuracy. Values of n much greater than 6 would require that J be $> 100 \text{ cm}^{-1}$, which seems physically unreasonable.

Physically, the condition $\Delta E \approx n\hbar\omega_1$ means that most of the electronic energy that must be removed from the reactants can be transferred into the n th-order vibration of the quantum mode in the products. When $n = 1$, small changes in d_1 do not disturb the energy matching greatly. The energy difference between ΔE and $\hbar\omega_1$ is readily made up by vibrations of the soft modes. When n is much greater than 1, an increase in d_1 causes a proportionately larger mismatching of the electronic and vibrational energy levels, and the rate decreases. This effect

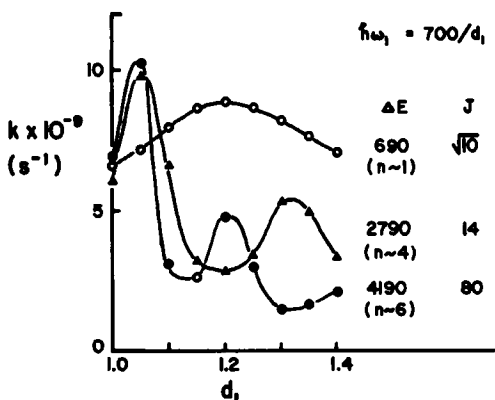


FIGURE 4 Theoretical dependence of k on the deuteration parameter d_1 at 300 K, for three different relationships between ΔE and $\hbar\omega_1$. For all three curves: $\hbar\omega_1 = 700/d_1$ cm^{-1} ; $\hbar\omega_2 = 50$ cm^{-1} ; $\hbar\omega_3 = 10$ cm^{-1} ; $S_1 = d_1$; $S_2, S_3, d_2, d_3 = 1.0$. The numbers to the right of the curves give ΔE and J in cm^{-1} . The ratio $n = \Delta E/\hbar\omega_1$ also is indicated.

is well known for other types of radiationless relaxation (35). The conclusion that $n > 1$ implies that the products of the electron transfer reaction must relax through more than one vibrational energy level of the quantum mode, after the electron transfer. The relaxation is significant, because it insures that the reaction will be effectively irreversible.

Studies of isotope effects in free-base porphyrins in solution have shown that the pyrrolic N—H bonds are particularly important in determining the rate of radiationless transitions from the triplet to the ground state (36, 37). Intersystem crossing is similar to electron transfer, in that Franck-Condon factors are important in both processes. The N—H bonds have vibrational bending modes near 700 cm^{-1} (38), which is the value used for $\hbar\omega_1$ in Figs. 3 B and 4, and an involvement of these bonds could explain the sensitivity of the kinetics to deuteration of the reaction centers. We do not know, however, whether the pyrrolic nitrogens were deuterated in the bacteriopheophytin of the ^2H reaction centers. Because the hydrogens on the pyrrolic nitrogens of free-base porphyrins are readily exchangeable in organic solution (38), one might expect that ^2H incorporated biosynthetically into these positions would be lost during the purification of the reaction centers. It is possible, however, that the bacteriopheophytins are buried in the hydrophobic interior of the reaction center, and are inaccessible to the solvent. Dialysis of ^1H reaction centers in $^2\text{H}_2\text{O}$ buffer had no effect on the rate constant, but this could mean either that the N—H groups do not exchange with the solvent, or that if they do exchange they have little influence on the kinetics. Studies with specifically deuterated reaction centers should prove informative.

We thank Dr. R. Blankenship for measuring the EPR linewidths, Dr. A. Warshel and Dr. R. Blankenship for helpful discussion, and Mr. J. Slater for assistance with reaction center preparation.

This work was supported by National Science Foundation grants PCM-79-02911 and PCM-77-13290-A02.

Received for publication 13 March 1981 and in revised form 29 July 1981.

REFERENCES

1. Holten, D., C. Hoganson, M. W. Windsor, C. C. Schenck, W. W. Parson, A. Migus, R. L. Fork, and C. V. Shank. 1980. Subpicosecond and picosecond studies of electron transfer intermediates in *Rhodopseudomonas sphaeroides* reaction centers. *Biochim. Biophys. Acta.* 592:461-477.
2. Shuvalov, V. A., and W. W. Parson. 1981. Energies and kinetics of radical pairs involving bacteriochlorophyll and bacteriopheophytin in bacterial reaction centers. *Proc. Natl. Acad. Sci. U.S.A.* 78:957-961.
3. Rockley, M. G., M. W. Windsor, R. J. Cogdell, and W. W. Parson. 1975. Picosecond detection of an intermediate in the photochemical reaction of bacterial photosynthesis. *Proc. Natl. Acad. Sci. U.S.A.* 72:2251-2255.
4. Kaufmann, K. J., P. L. Dutton, T. L. Netzel, J. S. Leigh, and P. M. Rentzepis. 1975. Picosecond kinetics of events leading to reaction center bacteriochlorophyll oxidation. *Science (Wash. D.C.)* 188:1301-1304.
5. Holten, D., M. W. Windsor, W. W. Parson, and J. P. Thornber. 1978. Primary photochemical processes in isolated reaction centers of *Rhodopseudomonas viridis*. *Biochim. Biophys. Acta.* 501:112-126.
6. DeVault, D., and B. Chance. 1966. Studies of photosynthesis using a pulsed laser. I. Temperature dependence of cytochrome oxidation rate in chromatium. Evidence for tunneling. *Biophys. J.* 6:825-847.
7. Parson, W. W. 1967. Flash-induced absorbance changes in *Rhodospirillum rubrum* chromatophores. *Biochim. Biophys. Acta.* 131:154-172.
8. Peters, K., P. Avouris, and P. M. Rentzepis. 1978. Picosecond dynamics of primary electron-transfer processes in bacterial photosynthesis. *Biophys. J.* 23:207-217.
9. Wraight, C. A., and R. K. Clayton. 1974. The absolute quantum efficiency of bacteriochlorophyll photooxidation in reaction centres of *Rhodopseudomonas sphaeroides*. *Biochim. Biophys. Acta.* 333:246-260.
10. Clayton R. K., and T. Yamamoto. 1976. Photochemical quantum efficiency and absorption spectra of reaction centers from *Rhodopseudomonas sphaeroides* at low temperature. *Photochem. Photobiol.* 26:67-70.
11. McElroy, J. D., D. C. Mauzerall, and G. Feher. 1974. Characterization of the primary reactions in bacterial photosynthesis. II. Kinetic studies of the light-induced EPR signal ($g = 2.0026$) and the optical absorbance changes at cryogenic temperatures. *Biochim. Biophys. Acta.* 333:261-277.
12. Hsi, E. S. P., and J. B. Bolton. 1974. Flash photolysis-electron spin resonance study of the effect of α -phenanthroline and temperature on the decay time of the ESR signal B1 in reaction-center preparations and chromatophores of mutant and wild type strains of *Rhodopseudomonas sphaeroides* and *Rhodospirillum rubrum*. *Biochim. Biophys. Acta.* 347:126-153.
13. Parson, W. W., R. K. Clayton, and R. J. Cogdell. 1975. Excited states of photosynthetic reaction centers at low redox potentials. *Biochim. Biophys. Acta.* 387:265-278.
14. Reynolds, W. L., and R. W. Lumry. 1966. Mechanisms of Electron Transfer. Ronald Press Co., New York.
15. Cogdell, R. J., T. G. Monger, and W. W. Parson. 1975. Carotenoid triplet states in reaction centers from *Rhodopseudomonas sphaeroides* and *Rhodospirillum rubrum*. *Biochim. Biophys. Acta.* 408:189-199.
16. Clayton, R. K., and R. T. Wang. 1971. Photochemical reaction centers from *Rhodopseudomonas sphaeroides*. *Methods Enzymol.* 23:696-704.
17. Wraight, C. A. 1979. Electron acceptors of bacterial photosynthetic reaction centers. II. H^+ binding coupled to secondary electron transfer in the quinone acceptor complex. *Biochim. Biophys. Acta.* 548:309-327.
18. Katz, J. J., R. C. Dougherty, H. L. Crespi, and H. H. Strain. 1966. Nuclear magnetic resonance studies of plant biosynthesis. A bacteriochlorophyll isotope mirror experiment. *J. Am. Chem. Soc.* 88:2856-2857.
19. Bevington, P. R. 1969. Data Reduction and Error Analysis for the Physical Sciences. McGraw-Hill Publications, New York.
20. Clayton, R. K., and H. F. Yau. 1972. Photochemical electron transport in photosynthetic reaction centers from *Rhodopseudomonas sphaeroides*. I. Kinetics of the oxidation and reduction of P-870 as affected by external factors. *Biophys. J.* 12:867-881.
21. Blankenship, R. E., and W. W. Parson. 1979. The involvement of iron and ubiquinone in electron transfer reactions mediated by reaction centers from photosynthetic bacteria. *Biochim. Biophys. Acta.* 545:429-444.
22. Jortner, J. 1980. Dynamics of the primary events in bacterial photosynthesis. *J. Am. Chem. Soc.* 102:6676-6686.
23. Redi, M., and J. J. Hopfield. 1980. Theory of thermal and photoassisted electron tunneling. *J. Chem. Phys.* 72:6651-6660.
24. DeVault, D. 1980. Quantum mechanical tunneling in biological systems. *Q. Rev. Biophys.* 13:387-564.
25. Blankenship, R. E., and W. W. Parson. 1979. Kinetics and thermodynamics of electron transfer in bacterial reaction centers. In Photosynthesis in Relation to Model Systems. J. Barber, editor. Elsevier Scientific Publishing Co., Amsterdam. 71-114.

26. Jortner, J. 1976. Temperature dependent activation energy for electron transfer between biological molecules. *J. Chem. Phys.* 64:4860-4867.
27. Lax, M. 1952. The Franck-Condon Principle and its application to Crystals. *J. Chem. Phys.* 20:1752-1760.
28. Kubo, R., and Y. Toyozawa. 1955. Application of the method of generating function to radiative and non-radiative transitions of a trapped electron in a crystal. *Prog. Theor. Phys.* 13:160-182.
29. Kakitani, T., and H. Kakitani. 1981. A possible new mechanism of temperature dependence of electron transfer in photosynthetic systems. *Biochim. Biophys. Acta.* 635:498-514.
30. Sarai, A. 1979. Energy gap and temperature dependences of electron transfer and excitation transfer in biological system. *Chem. Phys. Lett.* 63:360-366.
31. Sarai, A. 1980. Possible role of protein in photosynthetic electron transfer. *Biochim. Biophys. Acta.* 589:71-83.
32. Warshel, A. 1980. Role of the chlorophyll dimer in bacterial photosynthesis. *Proc. Natl. Acad. Sci. U.S.A.* 77:3105-3109.
33. Arata, H., and W. W. Parson. 1981. Delayed fluorescence from *Rhodopseudomonas sphaeroides* reaction centers: enthalpy and free energy changes accompanying electron transfer from P₈₇₀ to quinones. *Biochim. Biophys. Acta.* In press.
34. Arata, H., and W. W. Parson. 1981. Enthalpy and volume changes accompanying electron transfer from P₈₇₀ to quinones in *Rhodopseudomonas sphaeroides* reaction centers. *Biochim. Biophys. Acta.* 636:70-81.
35. Henry, B. R., and W. Siebrand. 1973. Radiationless transitions. In *Organic Molecular Photophysics*. J. B. Birks, editor. John Wiley & Sons Ltd., London. 1:153-237.
36. Burgner, R. P., and A. M. Ponte Goncalves. 1974. Deuterium isotope effect on the radiationless decay of the lowest triplet state of a porphyrin free base. *J. Chem. Phys.* 60:2942-2943.
37. Ponte Goncalves, A. M., and R. P. Burgner. 1977. Position-dependent deuterium isotope effects on the radiationless decay of the triplet state of porphyrin free bases. *Chem. Phys. Lett.* 46:275-278.
38. Mason, S. F. 1958. The infrared spectra of *N*-heteroaromatic systems. I. The porphins. *J. Chem. Soc. (Lond.)*. 976-982.